Passivated rear contacts for high-efficiency n-type Si solar cells providing high interface passivation quality and excellent transport characteristics

Frank Feldmann*, Martin Bivour, Christian Reichel, Martin Hermle, Stefan W. Glunz

Fraunhofer ISE, Heidenhofstr. 2, D-79110 Freiburg, Germany

ARTICLE INFO

ABSTRACT

In this work passivated rear contacts are used to replace point contact passivation schemes for high-efficiency n-type crystalline silicon solar cells. Our structure is based on an ultra-thin tunnel oxide (SiO_2) and a phosphorus-doped silicon layer, which significantly reduce the surface recombination at the metal–semiconductor interface. The passivation and transport mechanisms of this passivated contact will be addressed within this paper. Particular consideration will be given to the tunnel oxide's impact on interface passivation and on the I–V characteristics of n-type Si solar cells featuring a boron-diffused emitter. It will be shown that the tunnel oxide is a vital part of this passivated contact and that it is required to achieve excellent interface passivation for both open-circuit and maximum power point (MPP) conditions (implied open-circuit voltage $iV_{oc} > 710$ mV and implied fill factor $iFF > 84\%$). It will also become clear that the transport barrier arising from the tunnel oxide does not constrict the majority carrier flow. Thus, a low series resistance is obtained, which in conjunction with the high iFF enables FFs well above 82%. Investigations on cell levels lead to an independently confirmed conversion efficiency of 23.0% for n-type cells with a boron-diffused emitter and the herein developed passivated rear contact, in which the efficiency is not limited by the electrical properties of our passivated contacts.

© 2013 Elsevier B.V. All rights reserved.

1. Introduction

In 1985 Yablonovich stated that an ideal solar cell should "be built in the form of a double heterostructure", which would place the absorber between two wide-gap materials of opposite doping [1]. These semi-permeable membranes must ensure that the electrochemical energy (splitting of the quasi-Fermi levels) is completely converted into electrical energy [2]. A famous example is the HIT solar cell [3], achieving very high conversion efficiencies by making use of a heterojunction based on the hydrogenated amorphous silicon (a-Si:H), which effectively suppresses recombination at the a-Si:H and crystalline silicon (c-Si) interface as well as at the metal contacts. However, the temperature restrictions of the a-Si:H layers require a dedicated back-end processing (low-temperature deposition of transparent conductive oxide (TCO) and metallization). A temperature-stable approach is based on semi-insulating polysilicon (SIPOS), which was originally used as a passivation layer for silicon devices [4] and thence successfully implemented as an emitter in heterojunction transistors [5]. Its potential for photovoltaics was demonstrated by Yablonovich's

SIPOS solar cell, which achieved an impressively high V_{oc} of 720 mV [1]. In addition to SIPOS, the herein proposed passivated contact is closely related to the polyemitter technology, which significantly enhanced current gains of bipolar junction transistors [6]. The successful commercial application of the polysilicon emitter technology in high-speed logic circuits in the 1980s urged some researchers to apply these polysilicon contacts to solar cells with the aim to boost V_{oc} [7,8,9].

Our approach, which we have called *TOPCon* (Tunnel Oxide Passivated Contact) is based on these prior approaches and consists of an ultra-thin tunnel oxide and a phosphorus-doped silicon layer. It offers a simple processing scheme which is compatible with high-temperature processes such as diffusion.

To obtain highly efficient passivated contacts for solar cells, the following three prerequisites are to be met: (i) excellent interface passivation, (ii) efficiently doped layers to maintain the quasi-Fermi level separation in c-Si (high V_{oc}), and (iii) an efficient majority carrier transport (high FFs). To study the performance of our passivated contacts, their interface passivation is tested for by lifetime measurements, and prerequisites (ii) and (iii) are investigated on n-type silicon solar cells with a diffused boron-doped emitter on the front side and the newly developed passivated contacts on the rear side. Furthermore, we examine the cell's light trapping scheme with a focus on an appropriate rear metallization.

---

* Corresponding author. Tel.: +49 761 4588 5287; fax: +49 761 4588 9250.
E-mail address: frank.feldmann@ise.fraunhofer.de (F. Feldmann).

Finally, the limitations arising from the front grid metallization are discussed and a solution is proposed to reach efficiencies well above 24%.
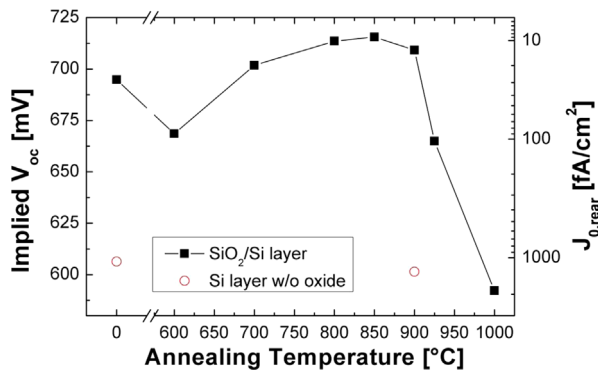
2. Experimental details and results

2.1. The interface passivation and its impact on device performance

The interface passivation quality of this passivated contact was determined on symmetrical lifetime samples by the quasi-steady-state photoconductance (QSSPC) technique [10]. Here, the implied open-circuit voltage iV_{oc} at one sun, which is calculated by

$$iV_{oc} = \frac{kT}{q} \ln\left(\frac{\Delta n (\Delta n + N_D)}{n_i^2}\right) \qquad (1)$$

is used as a measure for interface passivation. Shiny-etched n-type $1\,\Omega\,cm$ (100)-oriented floating zone (FZ) silicon wafers with a thickness of $200\,\mu m$ were cleaned according to the RCA cleaning procedure [11]. Then an ultra-thin wet chemical oxide layer was grown with a thickness determined to be about 14 Å by spectroscopic ellipsometry. It should be noted, that 20 Å is the maximum tolerable oxide thickness for the related metal–insulator–semiconductor (MIS) solar cells at which tunneling becomes inefficient and, thus, results in a lowered FF [12]. Subsequently, a 20 nm thick phosphorus-doped Si layer was deposited on both sides. Afterwards, the samples' passivation was activated in a tube furnace process with plateau temperatures in the range of $600\,°C < T_{anneal} < 1000\,°C$. Fig. 1 plots the iV_{oc} at 1 sun over T_{anneal}. It can be seen that a good passivation can be obtained already after deposition of the Si layer. Depending on the annealing conditions, the good initial passivation can be further boosted to very high implied voltages (iV_{oc} well above 710 mV). To relate our achievements with results from prior art, the corresponding $J_{0,rear}$ values of lifetime samples with $iV_{oc} > 710\,mV$ were determined using the method proposed by Kane and Swanson [13]. $J_{0,rear}$ values in the range of 9–13 fA/cm² were measured and show that our passivated contacts perform equally well as SIPOS (10 fA/cm²) [1] and as polyemitters with deliberately grown interfacial oxide (20 fA/cm²) [9].

For $T_{anneal} > 900\,°C$, a strong decrease in the interface passivation is observed. This can be explained with the local disruption of the SiO_2 tunnel junction in oxygen-free ambient according to the reaction $SiO_2(s) + Si(s) \rightarrow 2\,SiO(g)$, where s and g denote the solid and gaseous phase, respectively. This balling-up of oxide was also observed for polyemitter devices with deliberately grown
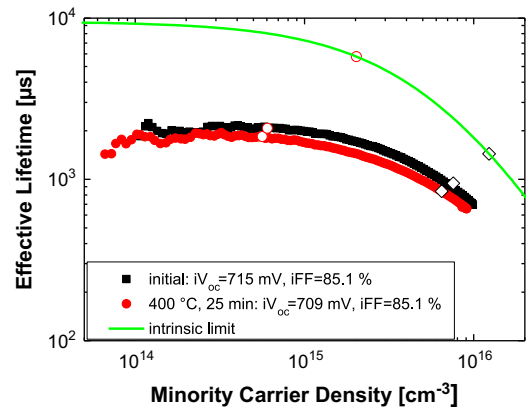
interfacial oxides [14] and inevitably leaves behind large areas of unpassivated silicon in direct contact with the Si layer. Notably, the tunnel oxide is crucial to obtain very high passivation quality, since lifetime samples solely passivated by an as-deposited Si layer or an annealed Si layer (red circles in Fig. 1) yield very low iV_{oc} values. A similar behavior for polyemitter contacts was observed by Kwark et al. [9].

Apart from a high V_{oc}, passivated contacts must also provide low interface recombination at MPP conditions to allow for high FFs [15]. Provided that the device would only be limited by Auger recombination, the upper limit for the fill factor FF_0 [16] is 89%. In Fig. 2 an injection-dependent effective minority carrier lifetime-curve $\tau_{eff}(\Delta n)$ is shown and the implied solar cell parameters iV_{oc} and iV_{MPP} are marked, respectively. The implied iV_{MPP} is obtained from the implied J–V curve calculated from the $\tau_{eff}(\Delta n)$ curve and can be understood as a similar measure for device performance as the PFF is for SunsVoc measurements [17]. While Auger recombination dominates at open-circuit (OC) conditions, the device does not operate close to the Auger limit at iV_{mpp}. However, a high implied fill factor iFF of about 85% is still obtained. To approach the ideal FF_0 of 89%, the interface passivation at MPP conditions must be even further enhanced to shift iV_{mpp} into the Auger recombination regime. The reduced passivation quality of the unpassivated lifetime samples (without tunnel oxide) leads thus not only to a lower iV_{oc} but also to a reduced iFF of about 83%.

While the passivated contact easily withstands typical diffusion temperatures, its interface passivation after the activation process should be stable at temperatures in the range of 400 °C to provide more opportunities for back-end processing. A typical process such as contact sintering and silicidation was simulated quite realistically by hotplate annealing of the symmetrical lifetime samples at 400 °C. In Fig. 2 it can be observed that the passivation quality and iV_{oc} values above 700 mV can be maintained during the applied annealing conditions. Thus, the passivated contact imposes fewer restrictions on back-end processing compared to classical a-Si:H based passivation schemes. A detailed study on the thermal stability, taking into account various TCO capping layers, will be performed in the future.

2.2. High-efficiency solar cells and transport characteristics

To investigate whether this passivated contact would be an efficient majority carrier contact, it was implemented at the rear side of n-type silicon solar cells with a diffused boron-doped

Fig. 1. The diagram depicts the implied V_{oc} of the *TOPCon*'s interface passivation as a function of the plateau temperature T_{anneal} of the furnace anneal. The samples without tunnel oxide (red circles) clearly underline the importance of the tunnel oxide layer for surface passivation. Additionally, the right y-axis depicts the corresponding $J_{0,rear}$ values calculated according to Eq. (3). (For interpretation of the references to color in this figure caption, the reader is referred to the web version of this article.)

Fig. 2. Measured injection dependent effective minority carrier lifetime for a sample symmetrically passivated by the *TOPCon* structure after thermal treatment at 800 °C and subsequent hotplate annealing at 400 °C for 25 min, respectively. The figure also depicts the open-circuit (1 sun, open diamonds) and MPP conditions (open circles) as well as the intrinsic limit of the absorber calculated according to [24].

emitter (140 Ω/sq) at the front side (see Fig. 3). The cells (2 × 2 cm²) were processed on n-type 1 Ω cm FZ silicon wafers. They feature a front surface with random pyramids and a passivated boron-diffused emitter. The 20 μm wide fingers were realized by thermal evaporation of a Ti/Pd/Ag seed layer and subsequent electroplating of Ag. The *TOPCon* structure at the rear surface was deposited and activated following emitter diffusion and drive-in anneal.

Table 1 lists the corresponding solar cell results for cells with passivated rear contacts and for those labeled "unpassivated" rear contacts, which do not employ the passivating tunnel oxide.

Most importantly, the tunnel oxide layer needed for passivation does not hinder majority charge carrier transport across its barrier and thus allows for excellent *FF*s of above 82%. From SunsVoc measurements [18] we obtained a *PFF* of 84.5%, which is the result of low device recombination at MPP conditions. The small difference between *PFF* and *FF* translates into a very low series resistance of $R_{S,SunsVoc}=0.41$ Ω cm², which is calculated according to [19]

$$R_{S,SunsVoc} = (PFF - FF)\frac{V_{oc}J_{sc}}{J_{mpp}^2}. \qquad (2)$$

Additionally, the light *I–V* method, which compares the light *I–V* curve with the J_{sc}-shifted dark *I–V* curve, was utilized to confirm the result obtained from the SunsVoc-method. Here, $R_{S,light}=0.37$ Ω cm² corroborates above calculation. The individual contributions to R_s can be easily identified by TLM measurements of the specific contact resistances in conjunction with simple spread-sheet calculations according to Goetzberger [20]. Due to a small pitch (800 μm) and silver's very low resistivity ($\rho_{met}=1.6$ μΩ cm), the lateral transport in the emitter and series resistance of the fingers make minor contributions ($R_{emitter}=0.08$ Ω cm² and $R_{finger}=0.07$ Ω cm²). On

the other hand, the grid's specific contact resistance ρ_c is determined to be as high as 9 mΩ cm², which translates into an upper value for the contact resistance at the diffused emitter of about 0.35 Ω cm². While the passivated contact's specific contact resistance takes a value of about 10 mΩ cm², its contribution to R_S can be neglected since the rear is fully metallized. Thus, the relatively small loss in *FF* due to series resistance can be solely attributed to the solar cell's front side.

While solar cells with point contact rear side passivation schemes (e.g. PERL) trade off V_{oc} for *FF* [21], the proposed passivated contact decouples the absorber's passivation from the metallization. Thus, the latter allows for a one-dimensional carrier transport in the base, thereby leading to a *FF* which is more than 1% absolute higher than the *FF* of a PERL solar cell featuring a similar front side [22]. Furthermore, the cells without oxide layer stress the importance of a low device recombination at MPP conditions. While the *FF* is absolutely 1% lower compared to the cells with the passivated rear contacts, the series resistance remains the same ($R_{S,SunsVoc}=0.40$ Ω cm²). Thus, the loss in *FF* can be ascribed to a lower *iFF* (as observed in Section 2.1) which reduces the *PFF* to 83.6%.

In addition to the high *FF*, a good V_{oc} as high as 691 mV can be obtained with this solar cell structure. In order to determine the weight of front and rear recombination, the J_0 value is calculated by

$$J_0 = J_{0,e} + J_{0,b} = J_{0,e} + J_{0,rear} + qn_i^2\frac{W}{N_D\tau_p}, \qquad (3)$$

where $n_i=8.3 \times 10^9$ cm^{-3} [23] and $t_p=3.4$ ms is the Auger lifetime after [24]. Although this analysis is only valid for low level injection conditions and, thus, prone to error in the case of n-type cells with $N_D=5 \times 10^{15}$ cm^{-3}, it is nevertheless a useful approximation unveiling the limiting factors. While the emitter is well passivated ($J_{oe,pass}=11$ fA/cm²), the unpassivated metal–semiconductor front contacts are the dominant source for recombination ($J_{oe,contact}=1800$ fA/cm²) and constitute an intrinsic loss mechanism of homojunction solar cells. With a metallized area fraction of about 3%, the total J_{oe} of 64 fA/cm² results in an upper limit ($J_{ob}=0$) for the cell's V_{oc} of about 700 mV. Taking into account the very low contribution of the rear contact ($J_{0,rear}=9$ fA/cm²) and the base (total $J_{0b}=22$ fA/cm²) to the cell's recombination current yields a V_{oc} of about 690 mV. Thus, the V_{oc} gap of > 20 mV between the solar cells and the lifetime samples can be mainly attributed to the recombination at the unpassivated metal–semiconductor front contacts.

As expected, the V_{oc} of the solar cells with an unpassivated contact (without tunnel oxide layer) is drastically decreased to 638 mV due to a high $J_{ob}=593$ fA/cm².

2.3. Light management at the rear side

In addition to a high V_{oc} and *FF*, a high-efficiency solar cell must have a transparent front side and an efficient light-trapping scheme, thus enhancing the optical path length within the absorber by several orders of magnitude. This is well done for
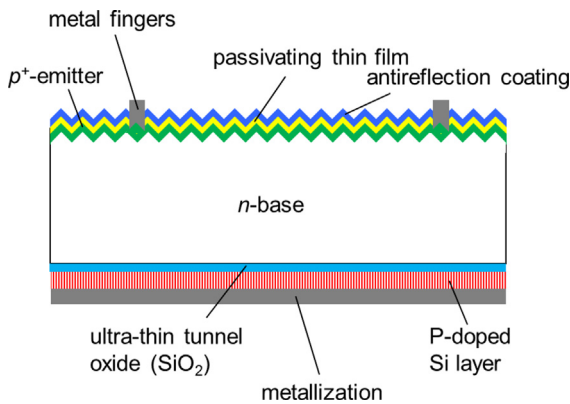
Fig. 3. Schematic of the solar cell structure with the passivated rear contact. The solar cells feature a diffused boron-doped emitter at the front side which is passivated by atomic layer deposited (ALD) aluminum oxide Al_2O_3 and a plasma-enhanced chemical vapor deposited (PECVD) silicon nitride SiN_x.
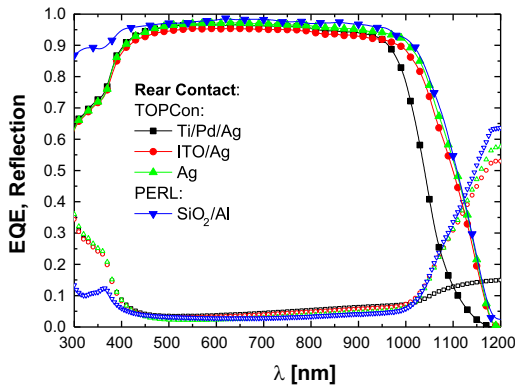
Table 1
I–V results of n-type solar cells featuring either a passivated rear contact or an unpassivated rear contact (w/o tunnel oxide layer) at the rear.

	V_{oc} (mV)	J_{sc} (mA/cm²)	*FF* (%)	*PFF* (%)	η (%)
Passivated rear contact					
Average (7 cells)	690.4 ± 0.9	38.4 ± 0.1	81.9 ± 0.2	84.5 ± 0.0	21.7 ± 0.1[a]
Best	**690.8**	**38.4**	**82.1**	**84.5**	**21.81**[a]
Unpassivated rear contact					
Average (7 cells)	637.7 ± 0.5	37.7 ± 0.1	81.2 ± 0.1	83.6 ± 0.0	19.5 ± 0.0
Best	**638.3**	**37.8**	**81.1**	**83.6**	**19.6**

[a] Solar cell results are independently confirmed by Fraunhofer ISE Callab.
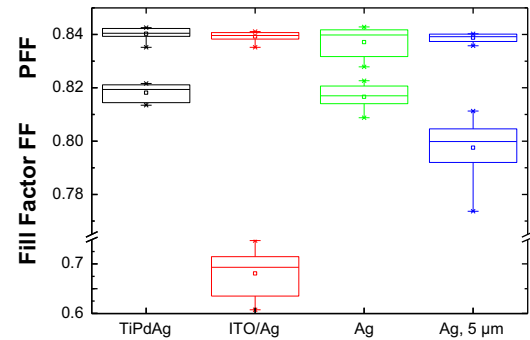
PERL solar cells, which feature a thick dielectric layer with a low index of refraction [22], ensuring that most light is totally reflected and not absorbed by the rear metallization. However, the application of any insulating dielectric layer would contradict the idea of our *TOPCon* structure and, thus, it would lose the inherent *FF* advantage of the one-dimensional junction design. Thus, the requirement for the rear contact in terms of internal reflection is quite high. The importance of a suitable rear side metallization is highlighted by our reference cell, where the rear is contacted by a stack of Ti/Pd/Ag. Here, the average short-circuit current J_{sc} is only 38.4 mA/cm², approximately 2–3 mA/cm² lower than that of a comparable PERL solar cell. The poor internal reflection of light at the rear side, as can be seen from the low reflectance in the range of 1000 nm $< \lambda <$ 1200 nm (see Fig. 4), can be explained by the absorption of evanescent waves at the metal surface. Thus, comparing the integrated EQE from 1000 nm to 1200 nm shows that there is a room for more than 2.8 mA/cm². To improve the internal reflection, a conductive back reflector (i.e. TCO) [25] with negligible absorption and/or a suitable metallization (i.e. Ag) [26] has to be implemented. Bivour et al. demonstrated that for a-Si:H (p) rear-emitter solar cells [26] Ag significantly increases the rear side reflection of cells with a textured front and planar rear. While this holds true for shiny-etched or polished surfaces, this is not the case for textured (or rough) rear surfaces [27], which are more common in heterojunction solar cells. Here, the Ag back reflector needs to be buffered from the Si layer by a TCO which does not absorb the evanescent waves. Recently, Holman et al. showed that the optimum thickness of the rear ITO layer is in the range of 150–200 nm, at which the evanescent waves can completely decay within the ITO layer and not get absorbed at the ITO/Ag interface [25]. To this end, similar solar cells were processed in which the Ti/Pd/Ag metal stack at the rear is replaced by a stack of a lowly doped 200 nm ITO/1 μm Ag and a single layer of 1 μm Ag, respectively.

The corresponding solar cell results are given in Table 2. The rear side reflection shown in Fig. 4 is significantly increased by applying the ITO/Ag stack and Ag single layer respectively. The light management of our passivated contacts in conjunction with the Ag single layer in particular is almost as good as the PERL reference and, thus, a very high J_{sc} of up to 40.1 mA/cm² is achieved. While both rear metallization schemes improve J_{sc}, only the cells with an Ag single layer achieve *FF*s above 82% (see Fig. 5). Contrary to this, the cells with the ITO/Ag stack suffer from a pronounced series resistance, thereby decreasing the *FF* below 75%. To further characterize the *FF* losses at the rear contact, which were also observed on a-Si:H(p) rear-emitter solar cells by Bivour et al. [28], TLM measurements of the contact resistances of Si layer/ITO and ITO/Ag are to be carried out in the future. In addition, the tiny decrease in V_{oc} can be ascribed to sputter damage of the interface passivation, which was also observed on lifetime samples (results not shown here).

Fig. 4. External quantum efficiency (lines and closed symbols) as well as the reflection (open symbols) of solar cells with different rear metallization schemes is plotted over wavelength. Titanium is a very loose metal and offers very weak reflection above 1000 nm. On the contrary, the stack of ITO/Ag reflects almost as much light as the Ag single layer. The best light management is obtained with our PERL cell (open symbols) [20] featuring a 100 nm SiO$_2$/Al mirror. Note, the cell's reflection in the wavelength range below 400 nm and between 600 and 1000 nm is slightly lower due to the use of inverted pyramids and a double antireflection coating.

Fig. 5. Pseudo-fill factor and fill factor are plotted for different rear metallization schemes (Ti/Pd/Ag, ITO/Ag, and Ag). Additionally, PFF and FF of the cells with Ag rear metallization and 5 μm (instead of 20 μm) contact opening on the front side (Ag, 5 μm) are given. The data reveals that the ITO/Ag stack introduces a pronounced series resistance effect while the Ag single makes good contact to the doped Si layer as well as the reference Ti/Pd/Ag does. The drop in FF for the solar cells with the smaller contact opening (Ag, 5 μm) on the front can be attributed to an increased contact resistance.

Table 2

I–V results of n-type solar cells featuring passivated rear contacts featuring either a stack of lowly doped ITO/Ag or a Ag single layer. In addition, the metallized area fraction of the front grid electrodes was varied.

	V_{oc} (mV)	J_{sc} (mA/cm²)	*FF* (%)	*PFF* (%)	η (%)
ITO/Ag at the rear, 20 μm contact opening					
Average (7 cells)	683.2 ± 1.8	39.3 ± 0.1	68.1 ± 4.4	83.9 ± 0.2	18.3 ± 1.1
Best	**681.8**	**39.1**	**74.7**	**83.5**	**19.9**
Ag at the rear, 20 μm contact opening					
Average (7 cells)	684.8 ± 2.4	39.5 ± 0.2	81.7 ± 0.4	83.7 ± 0.5	22.1 ± 0.3
Best	**687.4**	**39.6**	**82.3**	**84.1**	**22.4**
Ag at the rear, 5 μm contact opening					
Average (7 cells)	696.0 ± 1.3	40.6 ± 0.1	79.8 ± 1.1	83.9 ± 0.2	22.5 ± 0.4[a]
Best	**698.1**	**40.6**	**81.1**	**84**	**23.02**[a]

[a] Solar cell results are independently confirmed by Fraunhofer ISE Callab.

2.4. Improving V_{oc}

As shown above, the V_{oc} of the reference cells is limited by the recombination at the metal–semiconductor front contacts. To further improve the V_{oc}, solar cells with contact openings measuring at just 5 μm in width, albeit with the same finger geometry (20 × 10 μm) were processed. Thus, the nominal metallized area fraction is reduced from a A_{metal} of approximately 3% to roughly 1.1%. Owing to a smaller J_{oe} of approximately 30 fA/cm², the V_{oc} is expected to be slightly above 700 mV. Compared to the calibrated cells with a 3% metallized area fraction (see Table 1), the V_{oc} is indeed 7 mV larger and comes close to the estimated value. However, the increased V_{oc} comes at the cost of FF which is on average 1.9% lower than the FF of the cells with 20 μm contact opening (see Fig. 5 and Table 2). This loss in FF can be solely attributed to an even increased contribution of the contact resistance beneath the metal fingers to the cell's aggregate series resistance ($R_{S,SunsVoc} = 0.79\ \Omega\ cm²$). Unless the contact resistance of the grid fingers is negligible ($\rho_c < 10\ \mu\Omega\ cm²$), there is always a trade-off between V_{oc} and FF. And more importantly, even a tiny metallized area fraction of about 1.1% reduces the upper limit for the V_{oc} by more than 10 mV ($A_{metal} = 0\%$: $V_{oc} \approx 714$ mV, $J_{oe} = 11$ fA/cm², $J_{ob} = 22$ fA/cm²). Therefore, to further increase the V_{oc} while maintaining high FFs > 82%, a passivated contact with opposite doping for the boron-doped emitter is to be developed.

3. Summary

A thermally stable passivated contact for the rear side base contact of n-type silicon solar cells has been presented. It has been shown that our *TOPCon* structure based on a tunnel oxide and phosphorus doped Si layer passivates the surface effectively for both MPP and OC conditions and enables the extraction of V_{oc}s higher than 710 mV. The related J_{0b} value is as low as 22 fA/cm². The solar cells with the *TOPCon* structure have shown excellent performance regarding V_{oc} and FF. Contrary to point contact rear side passivation schemes like PERL, its one-dimensional design facilitates processing (no structuring and alignment) and enables high FFs above 82% while maintaining a high V_{oc}. The best cell has an independently confirmed efficiency of 23.0%. It has also been demonstrated that the efficiency is limited by the recombination at the unpassivated metal–semiconductor front contacts and that a viable solution would be a passivated contact for the boron-doped homojunction emitter. Such technology should further increase the efficiency of this solar cell concept well above 24%.

Acknowledgment

References

[1] E. Yablonovitch, T. Gmitter, R.M. Swanson, Y.H. Kwark, A 720 mV open circuit voltage SiO$_x$:c-Si:SiO$_x$ double heterostructure solar cell, Applied Physics Letters 47 (1985) 1211–1213 http://ieeexplore.ieee.org/xpls/abs_all.jsp?arnumber=4854043.

[2] P. Würfel, Physics of Solar Cells – From Principles to New Concepts, Wiley-Vch Verlag GmbH & Co KgaA, Weinheim, 2005.

[3] T. Kinoshita, D. Fujishima, A. Yano, A. Ogane, S. Tohoda, K. Matsuyama, Y. Nakamura, N. Tokuoka, H. Kanno, H. Sakata, M. Taguchi, E. Maruyama, The approaches for high efficiency HIT™ solar cell with very thin (< 100 μm) silicon wafer over 23%, in: Proceeding of the 26th EU-PVSEC, Hamburg, Germany, 2011, pp. 871–874.

[4] T. Aoki, T. Matsushita, H. Yamoto, H. Hayashi, M. Okayama, Y. Kawana, Oxygen-doped polycrystalline silicon films applied to surface passivation, Journal of the Electrochemical Society 122 (1975). (C82–C82).

[5] T. Matsushita, N. Ohuchi, H. Hayashi, H. Yamoto, Silicon heterojunction transistor, Applied Physics Letters 35 (1979) 549–550.

[6] I.R.C. Post, P. Ashburn, G.R. Wolstenholme, Polysilicon emitters for bipolar transistors: a review and re-evaluation of theory and experiment, IEEE Transactions on Electron Devices 39 (1992) 1717–1731.

[7] N.G. Tarr, A polysilicon emitter solar cell, IEEE, Electron Device Letters 6 (1985) 655–658 http://ieeexplore.ieee.org/xpls/abs_all.jsp?arnumber=1485417.

[8] F.A. Lindholm, A. Neugroschel, M. Arienzo, P.A. Iles, Heavily doped polysilicon-contact solar cells, IEEE, Electron Device Letters 6 (1985) 363–365.

[9] Y.H. Kwark, R.M. Swanson, N-type sipos and poly-silicon emitters, Solid State Electronics 30 (1987) 1121–1125.

[10] R.A. Sinton, A. Cuevas, M. Stuckings, Quasi-steady-state photoconductance, a new method for solar cell material and device characterization, in: Proceedings of the 25th IEEE Photovoltaic Specialists Conference, IEEE, New York, NY, USA, 1996, pp. 457–460.

[11] W. Kern, The evolution of silicon wafer cleaning technology, Journal of the Electrochemical Society 137 (1990) 1887–1892.

[12] J. Shewchun, R. Singh, M.A. Green, Theory of metal–insulator–semiconductor solar cells, Journal of Applied Physics 48 (1977) 765.

[13] D.E. Kane, R.M. Swanson, Measurement of the emitter saturation current by a contactless photoconductivity decay method (silicon solar cells), in: Proceedings of the 18th IEEE Photovoltaic Specialists Conference, Las Vegas, Nevada, USA, 1985, pp. 578–583.

[14] G.R. Wolstenholme, N. Jorgensen, P. Ashburn, G.R. Booker, An investigation of the thermal stability of the interfacial oxide in polycrystalline silicon emitter bipolar transistors by comparing device results with high-resolution electron microscopy observations, Journal of Applied Physics 61 (1987) 225–233.

[15] M. Reusch, M. Bivour, M. Hermle, S.W. Glunz, Fill Factor Limitation of Silicon Heterojunction Solar Cells by Junction Recombination, SiliconPV, Energy Procedia, Hamelin, Germany, 2013.

[16] M.A. Green, Accuracy of analytical expressions for solar cell fill factors, Solar Cells 7 (1981) 337–340.

[17] R.A. Sinton, A. Cuevas, A quasi-steady-state open-circuit voltage method for solar cell characterization, in: H. Scheer, B. McNelis, W. Palz, H.A. Ossenbrink, P. Helm (Eds.) Proceedings of the 16th European Photovoltaic Solar Energy Conference, James & James, London, UK, 2000, Glasgow, UK, 2000, pp. 1152–1155.

[18] R.A. Sinton, A. Cuevas, Contactless determination of current–voltage characteristics and minority–carrier lifetimes in semiconductors from quasi-steady-state photoconductance data, Applied Physics Letters 69 (1996) 2510–2512.

[19] D. Pysch, A. Mette, S.W. Glunz, A review and comparison of different methods to determine the series resistance of solar cells, Solar Energy Materials and Solar Cells 91 (2007) 1698–1706.

[20] A. Goetzberger, J. Knobloch, B. Voss, Crystalline silicon solar cells, John Wiley & Sons Ltd., Chichester, UK, 1998.

[21] S. Sterk, J. Knobloch, W. Wettling, Optimization of the rear contact pattern of high-efficiency silicon solar cells with and without local back surface field, Progress in Photovoltaics: Research and Applications 2 (1994) 19–26.

[22] J. Benick, B. Hoex, M.C.M. van de Sanden, W.M.M. Kessels, O. Schultz, S.W. Glunz, High efficiency n-type Si solar cells on Al$_2$O$_3$-passivated boron emitters, Applied Physics Letters 92 (2008) 253504/253501–253503.

[23] K. Misiakos, D. Tsamakis, Accurate measurements of the silicon intrinsic carrier density from 78-K to 340-K, Journal of Applied Physics 74 (1993) 3293–3297.

[24] A. Richter, F. Werner, A. Cuevas, J. Schmidt, S.W. Glunz, Improved parameterization of Auger recombination in silicon, Enrgy Proced 27 (2012) 88–94.

[25] Z.C. Holman, A. Filipič, A. Descoeudres, S. De Wolf, F. Smole, M. Topič, C. Ballif, Infrared light management in high-efficiency silicon heterojunction and rear-passivated solar cells, Journal of Applied Physics 113 (2013) 013107–013113 http://jap.aip.org/resource/013101/japiau/v013113/i013101/p013107_s013101.

[26] M. Bivour, C. Reichel, M. Hermle, S.W. Glunz, Improving the a-Si:H(p) rear emitter contact of n-type silicon solar cells, Solar Energy Materials and Solar Cells 106 (2012) 11–16 http://www.sciencedirect.com/science/article/pii/S092702481200339X.

[27] S.K. Kim, H.S. Ee, W. Choi, S.H. Kwon, J.H. Kang, Y.H. Kim, H. Kwon, H.G. Park, Surface-plasmon-induced light absorption on a rough silver surface, Applied Physics Letters 98 (2011).

[28] M. Bivour, C. Meinhardt, D. Pysch, C. Reichel, K.U. Ritzau, M. Hermle, S.W. Glunz, n-type silicon solar cells with amorphous/crystalline silicon heterojunction rear emitter, in: Proceedings of the 35th IEEE Photovoltaic Specialists Conference, Honolulu, Hawaii, USA, 2010.